Article

Not peer-reviewed version

Phosphate Mining Residues as Novel Substrate for Advanced Vertical Flow Constructed Wetlands: A Circular Economy Approach

Meryem Hdidou , Mohamed Chaker Necibi , Jérôme Labille , Amal An-nori , Bouchaib Gourich , Nicolas Roche *

Posted Date: 29 April 2026

doi: 10.20944/preprints202604.2002.v1

Keywords: constructed wetlands; heavy metals; mining residues; reactive media; water reuse; wastewater treatment; water loss

Article

Phosphate Mining Residues as Novel Substrate for Advanced Vertical Flow Constructed Wetlands: A Circular Economy Approach

Meryem Hdidou [1], Mohamed Chaker Necibi [1], Jérôme Labille [2], Amal An-nori [3], Bouchaib Gourich [1,4] and Nicolas Roche [1,2,*]

[1] International Water Research Institute (IWRI), Mohammed VI Polytechnic University, Ben Guerir 43150, Morocco

[2] CNRS, IRD, INRAE, Coll France, CEREGE, Aix-Marseille University, 13454 Aix en Provence, France

[3] Agricultural Innovation and Technology Transfer Center (AITTC), Mohammed VI Polytechnic University, Benguerir 43150, Morocco

[4] Laboratory of Process and Environmental Engineering, Higher School of Technology, Hassan II University of Casablanca, Morocco

* Correspondence: nicolas.roche@um6p.ma or nicolas.roche@univ-amu.fr

Abstract

Constructed wetlands offer a sustainable, decentralized solution for wastewater treatment and reuse in Morocco. This study evaluated mesocosm-scale advanced vertical flow constructed wetlands (AVFCWs) incorporating locally sourced reactive media to assess phosphate mining residues as a novel substrate. Accordingly, four configurations were compared: a sand-based control (CW-A) and three amended systems combining pozzolan with phosphate mining residues (CW-B), clay (CW-C), and biochar (CW-D), operated in batch mode under hydraulic retention times (HRTs) of 24, 48, and 72 h. The incorporation of reactive media significantly improved treatment efficiency, with CW-D achieving high removal efficiencies across most parameters. COD and TSS removal reached 80% and 88%, respectively, while nitrogen removal exceeded 82% in optimal configurations. Phosphorus removal reached 76% in CW-B and 88% in CW-C. The removal of Cd and Cu exceeded 85% in all systems, with phosphate mining residues demonstrating strong potential for metal immobilization. However, despite these high removal efficiencies, the treated effluent did not meet Moroccan reuse standards for cadmium and faecal coliforms, indicating that single-stage AVFCWs are insufficient for safe agricultural reuse and require additional polishing steps. Extended HRT improved AVFCWs performance, but increased water loss, reaching up to 28% due to evapotranspiration. Hence, phosphate mining residues emerge as promising substrate, pending further optimization, while supporting circular economy objectives.

Keywords: constructed wetlands; heavy metals; mining residues; reactive media; water reuse; wastewater treatment; water loss

1. Introduction

Global water use has been consistently increasing by approximately 1% per year over the past four decades, a trend projected to continue through 2050. This increase is mainly driven by population growth, socio-economic development, and shifting consumption patterns [1]. At the same time, climate change is intensifying droughts particularly in vulnerable regions such as the Mediterranean [2]. These combined pressures are exacerbating water scarcity. In parallel, the discharge of untreated or inadequately treated wastewater has emerged as a significant source of water pollution threatening aquatic ecosystems and human health. To address this situation, the reuse of treated wastewater has gained recognition as a sustainable water management strategy,

 doi:10.20944/preprints202604.2002.v1

particularly in arid and semi-arid regions. Therefore, reusing treated effluents in agriculture, which accounts for over 72% of global freshwater consumption, has been adopted in several countries [1]. Reclaimed wastewater not only provides an alternative water source but also contains valuable elements such as nutrients and organic matter [3,4]. However, long-term use of treated wastewater for irrigation raises significant environmental and public health concerns due to the bioaccumulation of persistent contaminants such as heavy metals and emerging pollutants. Unlike organic pollution, the removal of these contaminants through conventional processes is minimal and require advanced processes for effective removal [5].

Constructed wetlands (CWs), a nature-based solution, offer an attractive pathway for decentralized wastewater treatment and agricultural reuse. In CWs, a variety of physical, chemical, and biological processes co-occur, enabling the removal of a wide range of contaminants [6]. CWs have the potential to achieve high performances in terms of organic matter and suspended solids removal, exceeding 90% at reasonable investment and operational costs [7,8]. However, one of their main limitations is the requirement for relatively long hydraulic retention times (HRTs) leading to a large surface area, which may limit the use of CWs for large wastewater volumes. Therefore, improving pollutant removal efficiency under shorter HRT is essential for improving the feasibility of CWs while ensuring high treatment performances that respect wastewater reuse standards. One promising approach involves replacing the traditional sand and gravel substrate with highly adsorptive media that enhance contaminant immobilization. The use of these materials enhances key removal mechanisms, such as adsorption, ion exchange, precipitation, and surface complexation, while increasing biofilm development fostered by their porous structure [9]. As a result, these reactive media can accelerate pollutant sequestration, enabling CWs to operate efficiently under shorter HRTs and higher hydraulic loading rates (HLRs), thereby reducing the overall footprint of the system.

In Morocco, several low-cost, locally available materials are of high interest for use in CWs, including biochar derived from local biomass waste; pozzolan, a highly porous volcanic raock; and clay minerals rich in cation exchange sites. While these materials have been investigated in CWs, phosphate mining residues, an abundant by-product of Morocco's strategic phosphate industry, remain completely unexplored, with no existing studies evaluating their potential use in CWs. These residues are generated in large volumes during the extraction process and are commonly stockpiled, occupying valuable land and presenting long-term environmental management challenges [10]. These residues are characterized by heterogeneous mineral composition dominated by fluorapatite, along with carbonate and clay minerals. These properties suggest strong potential for water treatment applications since it promotes several removal mechanisms. The high calcium content is expected to support Ca-P precipitation, enhancing phosphorus removal [11,12]. In addition, metals can be removed through adsorption, ions exchange, precipitation and complexation [13]. And finally, the alkaline character of these materials may contribute to metal immobilization by supporting the formation of metal hydroxides and carbonates [14].

In addition, their valorization contributes to a circular economy approach by transforming a problematic industrial by-product into a valuable resource for sustainable wastewater treatment systems.

Accordingly, this study aims to provide a first evaluation of phosphate mining residues as a CWs substrate. Given their properties, these residues are expected to enhance treatment efficiency of CWs, potentially achieving performance comparable to that of established reactive media such as clay and biochar, while operating under shorter HRTs and thereby reducing the systems footprint. To explore this potential, a mesocosm-scale experiment was conducted to compare four single-stage advanced vertical flow CWs (AVFCWs): a conventional sand-based control and three amended systems incorporating phosphate mining residues, clay, pozzolan and biochar. The specific objectives of this research are to: (i) evaluate the efficiency of AVFCWs mesocosms amended with a combination of different reactive media in removing conventional contamination in addition to heavy metals; (ii) to compare the role of the different materials on the removal of the contaminants; (iii) to study the effect of HRT on the treatment efficiency; (iv) to evaluate water loss driven by evapotranspiration

 doi:10.20944/preprints202604.2002.v1

under semi-arid to arid condition; and (v) to assess effluent quality regarding Moroccan reuse standards to identify achievable targets and parameters requiring additional polishing steps.

2. Materials and Methods

2.1. AVFCW Mesocosms Configuration

The experiments were conducted in the greenhouse of the UM6P experimental farm in Benguerir, Morocco, from June to December 2024. The AVFCW mesocosms were constructed using cylindrical plastic containers (30 cm × 50 cm; diameter × Height) with a surface area of 0.07 m^2, as shown in Figure 1. The experimental setup aimed to evaluate the effect of incorporating the different reactive media, as well as their combined effects, on the removal of organic and inorganic contaminants from domestic wastewater. Hence, four AVFCW mesocosms, labelled: CW-A (control), CW-B, CW-C and CW-D, were implemented using various combinations of substrate materials. The arrangement, depth, and material ratios of each substrate layer are summarized in Table 1. The layer arrangement and substrate configuration were selected based on vertical flow constructed wetland design principles, with each layer fulfilling a specific hydraulic and treatment function. The reactive materials were chosen according to their physicochemical properties, local availability, and circular economy potential, while the mixture ratios were defined based on preliminary batch and continuous adsorption tests to balance treatment performance with hydraulic conductivity. All systems included a 10 cm gravel drainage layer at the bottom. In the control system CW-A, the drainage layer was topped with 34 cm of fine sand. CW-B and CW-C consisted of four layers, arranged from bottom to top as follows: drainage layer, a 12 cm layer consisting of a mixture of biochar and pozzolan, a 12 cm layer consisting of a mixture of pozzolan and mining residues (CW-B) or pozzolan and clay (CW-C) and finally a 10 cm layer of sand. CW-D, on the other hand, consisted of three layers: a drainage layer, a 24 cm layer comprising a mixture of biochar and pozzolan and a 10 cm layer of sand at the top. Pozzolan was systematically combined with all tested reactive media to maintain adequate hydraulic conductivity. A geotextile was placed between the layers to prevent fine particles from being washed out with wastewater. Subsequently, each AVFCW mesocosm was planted with two young Arundo Donax plants. Before starting the experiments, the AVFCWs underwent a two-month acclimation period. During the first month, the systems were irrigated with freshwater to support plant growth and maturation. In the second month, they were conditioned with wastewater to promote the development and maturation of microbial biofilm within the substrate. This allowed the establishment of diverse microbial communities essential for biological processes and helped ensure consisting operating conditions.

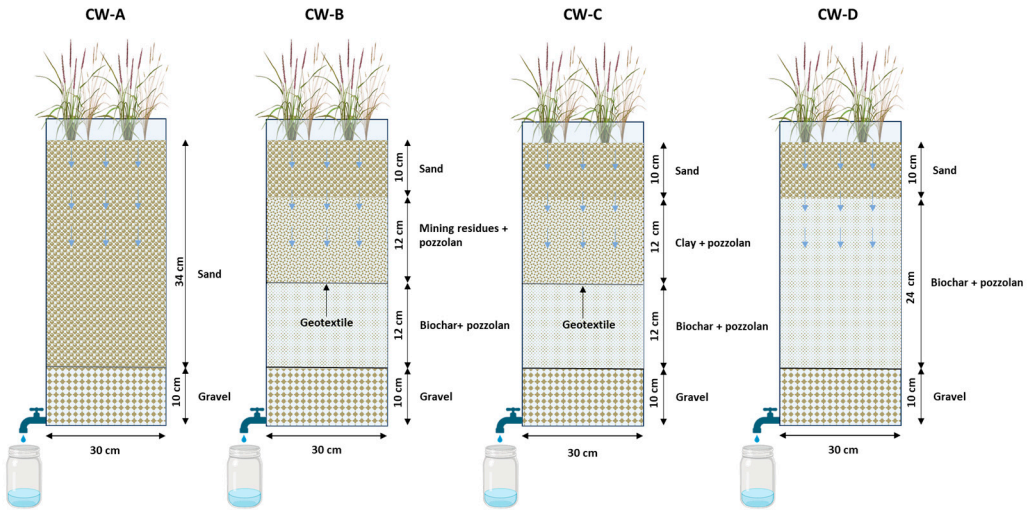

Figure 1. Schematic diagram of experimental constructed wetland systems.

 doi:10.20944/preprints202604.2002.v1

Table 1. Characteristics and disposition of the materials in the CW mesocosms.

CWs Label	Layers	Layer depth (cm)	Substrate materials	Mixture ratios (w:w)
CW-A	1st layer	34	Sand silex	100
	2nd layer	10	Gravel	100
CW-B	1st layer	10	Sand silex	100
	2nd layer	12	Pozzolan: Mining residues	80:30
	3rd layer	12	Pozzolan: biochar	70:30
	4th layer	10	Gravel	100
CW-C	1st layer	10	Sand silex	100
	2nd layer	12	Pozzolan: clay	70:30
	3rd layer	12	Pozzolan: biochar	70:30
	4th layer	10	Gravel	100
CW-D	1st layer	10	Sand silex	100
	2nd layer	24	Pozzolan: biochar	70:30
	3th layer	10	Gravel	100

2.2. Reactive Media Characterisation

The reactive media used in this study were characterized to understand their physicochemical properties and potential removal mechanisms. Mineralogical composition was determined by X-ray diffraction using Co Kα radiation (2θ 5–75°) (XRD, PANalytical X'Pert PRO). Surface morphology and elemental composition were provided by Scanning electron microscopy (SEM, JEOL JSM-7100F) coupled with energy dispersive X-ray spectroscopy (EDS, JSM-IT200). Samples were gold-coated before analysis. Specific surface area was determined using the Brunauer-Emmett-Teller (BET, Micromeritics 3Flex 5.02.01) method with N_2 adsorption at 77K. The materials pH was measured in deionized water (1:20 (*w*/*v*)) after one hour equilibration [15].

2.3. Operation of the Experimental Setup

Primary-treated wastewater was collected from the wastewater treatment plant (WWTP) of Benguerir and stored in a 1000-litre inlet tank. To evaluate the simultaneous removal of organic and inorganic contaminants, the wastewater was spiked with high concentrations of cadmium (Cd 0.8-1.2 mg/L) and copper (Cu: 1.2-2.0 mg/L) compared with those found in typical domestic wastewater. This challenge load approach was adopted to evaluate the adsorption and immobilization of pollutants under more stringent conditions. The selected concentrations were therefore intended to stress the AVFCW mesocosms, enabling clearer differentiation of their removal capacities. To ensure wastewater homogenisation, a closed-loop recirculation system was installed in the storage tank using a submersible pump. The AVFCW mesocosms were operated in batch feeding mode, where every cycle consisted of influent feeding, retention time, and drainage. For each cycle, an influent volume of 10 litres was loaded onto the surface of each mesocosm using a peristaltic pump at a flow rate of 2 L/min. Drainage was conducted by opening a valve located at the bottom of the mesocosm after the designated retention time. The experiments were conducted in three phases to assess the impact of HRT on treatment efficiency: phase (I) with an HRT of 24 h, and four cycles per week; phase (II) with an HRT of 48 h, and three cycles per week; and phase (III) with an HRT of 72 h, and two cycles per week. Each phase lasted four weeks. As the three phases were conducted sequentially from June to December, ambient temperature declined across the experimental period, with average values of 24.01 °C, 20.08 °C, and 14.09 °C in Phases I, II, and III, respectively.

 doi:10.20944/preprints202604.2002.v1

2.4. Water Sampling and Analysis

In situ measurements, including electrical conductivity (EC), pH, temperature (T°), and dissolved oxygen (DO), were performed using portable meters (Eutech™ PC 450 Multi-Parameter Meter and inoLab® Oxi 7310 Oximeter). Samples from the inlet and outlet of the AVFCW mesocosms were collected during each treatment cycle using sterilised polyethylene bottles. The samples were immediately transported to the laboratory and stored at 4 °C until analysis. The samples were analysed by the Agricultural Innovation and Technology Transfer Center laboratory (AITTC, UM6P-BENGUERIR) for chemical oxygen demand (COD), total suspended solids (TSS), total phosphorus (TP), total nitrogen (TN), copper (Cu), and cadmium (Cd). The COD concentration was determined by spectrophotometry, after oxidising the samples with potassium dichromate in a strongly acidic medium (sulfuric acid) at high temperatures. TSS was determined by filtering a sample through a 0.45 µm membrane, drying the membrane at 105 °C, and weighing it before and after filtration. The TSS concentration was calculated based on the mass difference. TN and TP were analysed using colorimetric methods with a continuous flow analyser (SAN^{++}, Skalar). Total concentrations of Cd and Cu were determined via inductively coupled plasma optical emission spectrometry (ICP-OES; Agilent 5110) following nitric acid digestion, without prior filtration. The faecal coliforms (FC) were enumerated, as specified in NM ISO 9308:2019, at Protège Maroc Laboratory (Casablanca). A sample volume was filtered through a 0.45 µm membrane to retain bacteria, then placed on a chromogenic coliform agar (CCA) plate. After incubation at 36 ± 2 °C for 21 ± 3 h, colonies were counted.

2.5. Water Balance and Evapotranspiration Estimation

The evapotranspiration (ET) rate from each mesocosm was estimated using the water balance method according to the equation [16]:

$$ET = {}^{Q_1}/_{A} + P - {}^{Q_2}/_{A} \quad (1)$$

where ET = Evapotranspiration rate (m^3/day), Q_1 = wastewater inflow rate (m^3/day), Q_2 = wastewater effluent rate (m^3/day), A = mesocosm surface area (m^2), P = precipitation rate (m/day)

In this study, P = 0 since the experimental setup was installed in a greenhouse, eliminating direct rainfall input. The influent volume was regulated using the peristaltic pump, while the effluent collected from each mesocosm was weighed using a scale to determine the volume of the treated water.

2.6. Statistical Analysis

The performance of the AVFCW mesocosms amended with different reactive media was statistically evaluated by comparing the mean effluent concentrations of selected physicochemical and biological parameters under the same hydraulic retention times (HRTs). The experimental design consisted of one mesocosm per substrate configuration, hence replications were achieved through successive batch treatment cycles within each phase. The effective sample sizes per treatment were n = 16 in phase I, n = 12 in phase II and n = 8 in phase III. Statistical analyses were conducted using IBM SPSS Statistics (Version 27). Normality and homogeneity of variance were assessed using the Shapiro-Wilk and Levene tests, respectively. When these assumptions were met, one-way ANOVA followed by Tukey test was applied; otherwise, the non-parametric Kruskal-Wallis test was used. Statistical significance was considered at a confidence level of $p < 0.05$. Principal component analysis (PCA) was performed on the entire standardized database to identify potential relationships between the variables and the underlying gradients governing the AVFCWs. Meanwhile, spearman correlation was applied to assess linear relationships among operational and effluent quality parameters. Spearman correlation was selected due to the non-normal distribution of several parameters.

 doi:10.20944/preprints202604.2002.v1

3. Results

3.1. Reactive Media Characterization

The XRD profile shown in Figure 2 reveals the mineralogical composition of the different adsorbents, agreeing with the elemental composition given by EDS analysis and presented in Figure S1. Mining residues were characterized by mineralogical heterogeneity dominated by Fluorapatite ($Ca_5(PO_4)_3F$) evidenced by high content of Ca, P and F. Small quantities of carbonate minerals (calcite and dolomite), Palygorskite and quartz are also present. The clay samples consist of Illite confirmed by the presence of Si, Al, K, and Fe with the presence of microcline, hematite and anatase phases. Pozzolan consists predominantly of an amorphous phase typical of volcanic rock, with the presence of minor crystalline phases dispersed throughout, namely olivine, pyroxene, and faujasite supported by diverse elemental composition (Si, Al, Fe and Ca). Biochar on the other hand displayed two broad diffraction peaks indicating the amorphous carbon phase. BET surface area analysis demonstrated that biochar exhibited relatively high specific surface area (366.15 m^2/g), followed by clay (26.77 m^2/g), phosphate mining residues (21.47 m^2/g), and pozzolan (15.69 m^2/g), all considerably higher than sand and gravel (<1 m^2/g) [17]. The pH values of the substrates ranged from 8.1 and 8.75 showing an alkaline character.

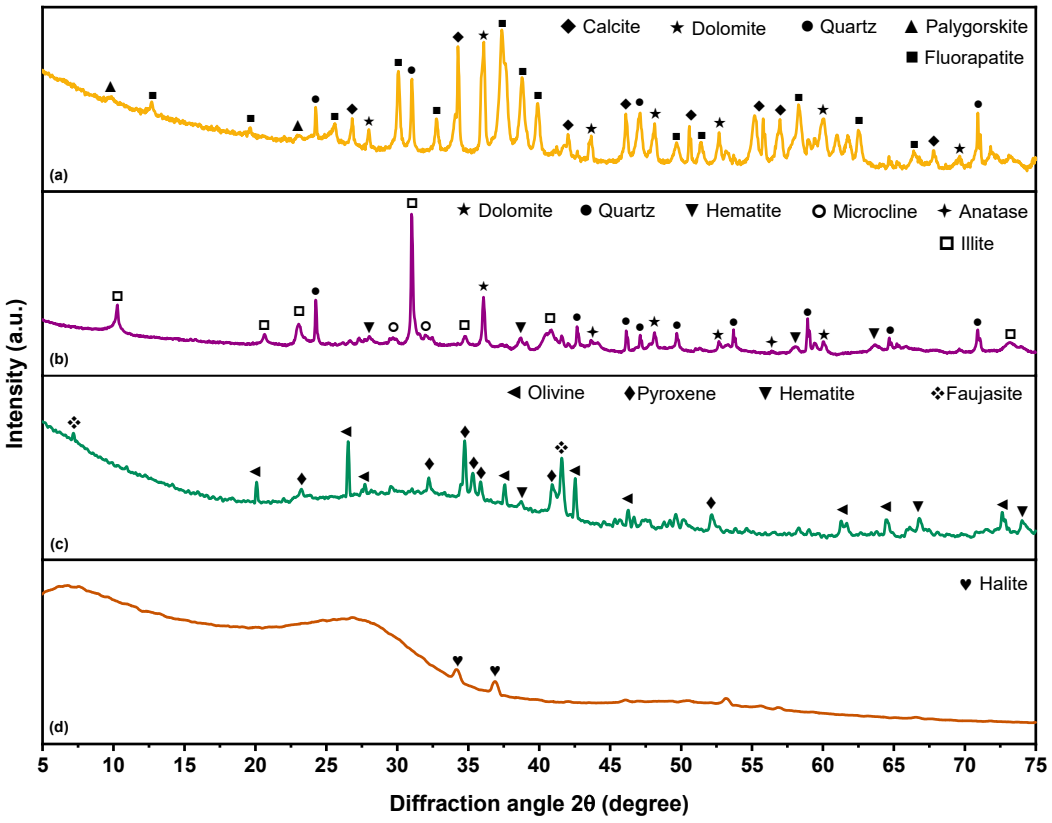

Figure 2. XRD patterns of (a) phosphate mining residues, (b) Clay, (c) Pozzolan, and (d) Biochar.

3.2. Environmental Parameters

Figure 3 displays influent-effluent pH, EC, DO, and temperature profiles across the AVFCWs during the three experimental phases.

pH

The pH of raw wastewater (RW) fluctuated throughout the experiment, with average values of 8.27 ± 0.29, 7.85 ± 0.67, and 7.69 ± 0.29 in phases I, II, and III, respectively. The effluent pH was reduced and stabilised to near neutral within all the AVFCW mesocosms as shown in Table 2 and Figure 3a.

 doi:10.20944/preprints202604.2002.v1

Electrical conductivity

The wastewater used in the present study is characterized by a relatively high electrical conductivity (EC), which remains stable through the experiment as shown in Figure 3b. A slight increase in the EC was observed in the effluent of all AVFCW mesocosms across the three phases with CW-A exhibiting the lowest EC. Furthermore, peaks in EC were observed after periods of AVFCW mesocosms inactivity likely indicating the accumulation of dissolved ions and their subsequent flushing when operation restarted.

Dissolved oxygen

The dissolved oxygen (DO) in the influent was significantly low compared to values reported in other studies [18,19] thereby minimizing oxygen supply from the influent. As shown in Table 2 and Figure 3-c, DO levels in the influent ranged from 0.83 ± 0.30 mg/L in phase I to 1.23 ± 1.21 mg/L in phase III. For all the AVFCW mesocosms, the effluent DO fluctuated over time with CW-A exhibiting the lowest values among all the mesocosms, with an average of 0.90 ± 0.39, 0.66 ± 0.31, and 1.03 ± 0.38 mg/L in phases I, II and III, respectively. According to the ANOVA test, there is a statistically significant difference in DO values between CW-A and the other AVFCWs ($p < 0.05$).

Temperature

The average influent temperatures were 25.8 ± 1.66 °C, 21.81 ± 2.17 °C, and 16.23 ± 2.68 °C in phases I, II, and III, respectively (Table 2, Figure 3-d). A clear declining trend was recorded across the experimental period, reflecting seasonal variation in ambient temperature, corresponding to an average of 24.01 °C in phase I, 20.08 °C in phase II and 14.09 °C in phase III.

Table 2. The average pollutants influent and effluent concentrations and removal efficiencies of the AVFCWs in the three phases (mean ± SD).

Parameters	Influent	CW-A	CW-B	CW-C	CW-D
Phase I					
pH	8.27 ± 0.29	7.60 ± 0.17a	7.44 ± 0.13a	7.48 ± 0.16a	7.48 ± 0.13a
EC (mS/cm)	3.19 ± 0.10	3.33 ± 0.14a	3.59 ± 0.40a	3.42 ± 0.21a	3.54 ± 0.34a
DO (mg/L)	0.83 ± 0.30	0.90 ± 0.39a	1.59 ± 0.33b	1.53 ± 0.30b	1.53 ± 0.31b
Temperature (°C)	25.8 ± 1.66	23.4 ± 1.31a	23.5 ± 1.23a	23.6 ± 1.29a	23.5 ± 1.28a
COD (mg/L)	243.96 ± 51.14	135.56 ± 25.65a	72.20 ± 19.28b	81.69 ± 26.76b	64.03 ± 18.15b
Re (%)		43.18 ± 11.27	69.72 ± 7.80	65.32 ± 13.16	72.90 ± 8.86
TSS (mg/L)	73.69 ± 15.79	18.69 ± 10.49a	8.44 ± 5.21b	8.69 ± 5.30b	9.56 ± 5.77b
Re (%)		74.72 ± 13.95	88.92 ± 5.63	88.62 ± 5.60	87.47 ± 6.01
TN (mg/L)	88.06 ± 8.06	76.70 ± 12.60a	47.92 ± 17.12b	42.50 ± 15.14b	40.02 ± 16.41b
Re (%)		13.35 ± 7.81	46.12 ± 17.59	52.35 ± 14.72	55.13 ± 17.17
TP (mg/L)	8.77 ± 0.79	7.18 ± 1.52a	2.04 ± 0.67 b	2.11 ± 0.84b	4.22 ± 1.11c
Re (%)		18.40 ± 13.83	76.41 ± 8.87	75.69 ± 10.11	51.41 ±14.07
Cu (mg/L)	1.66 ± 0.21	0.36 ± 0.16a	0.3 ± 0.15a	0.29 ± 0.14a	0.3 ± 0.14a
Re (%)		78.69 ± 7.84	82.30 ± 6.87	83.10 ± 6.12	82.50 ± 6.33
Cd (mg/L)	1.19 ± 0.15	0.28 ± 0.11a	0.14 ± 0.06b	0.14 ± 0.07b	0.14 ± 0.06b
Re (%)		76.20 ± 9.83	87.82 ± 5.26	88.02 ± 4.77	88.57 ± 4.69
FC (Log CFU/100mL)	4.90 ± 0.96	3.62 ± 1.30a	1.78 ± 1.44b	1.97 ± 1.53b	1.48 ± 1.48b
Re (Ulog)		1.27 ± 1.11	3.08 ± 1.69	2.92 ± 1.62	3.42 ± 1.44
Phase II					
pH	7.85 ± 0.67	7.24 ± 0.23a	7.15 ± 0.18 a	7.08 ± 0.18a	7.14 ± 0.17a
EC (mS/cm)	3.13 ± 0.05	3.28 ± 0.14a	3.47 ± 0.31a	3.55 ± 0.24a	3.41 ± 0.21a
DO (mg/L)	0.99 ± 0.63	0.66 ± 0.31a	1.24 ± 0.40b	1.41 ± 0.39b	1.21 ± 0.31b
Temperature (°C)	21.81 ± 2.17	20.23 ± 2.04a	19.97 ± 2.04a	20.37 ± 2.07a	19.89 ± 1.97a
COD (mg/L)	294.29 ± 80.44	143.98 ± 30.25a	86.02 ± 35.14b	73.61 ± 34.87b	61.52 ± 38.43b
Re (%)		49.56 ± 10.56	70.18 ± 10.71	74.14 ± 12.90	79.13 ± 10.57
TSS (mg/L)	72.83 ± 31.27	23.25 ± 13.57a	8.33 ± 2.42b	8.08 ± 3.92b	8.33 ± 3.60b

 doi:10.20944/preprints202604.2002.v1

Re (%)		67.97 ± 13.47	87.64 ± 4.21	88.04 ± 6.00	87.73 ± 5.98
TN (mg/L)	72.68 ± 6.65	58.26 ± 3.83a	34.40 ± 13.92b	36.81 ± 12.18b	27.99 ± 13.97 b
Re (%)		19.32 ± 8.34	53.48 ± 14.59	49.79 ± 14.20	62.47 ± 14.21
TP (mg/L)	7.01 ± 1.60	5.88 ± 1.71a	2.37 ± 0.54b	2.40 ± 0.82b	4.03 ± 0.51c
Re (%)		16.78 ± 11.21	65.71 ± 6.52	64.82 ± 12.28	40.51 ± 11.09
Cu (mg/L)	1.22 ± 0.29	0.26 ± 0.14a	0.21 ± 0.11a	0.14 ± 0.10a	0.17 ± 0.10a
Re (%)		76.91 ± 13.25	83.06 ± 7.07	88.56 ± 6.73	85.14 ± 7.48
Cd (mg/L)	0.75 ± 0.12	0.13 ± 0.11a	0.08 ± 0.03ab	0.06 ± 0.02b	0.06 ± 0.02b
Re (%)		83.93 ± 10.63	89.08 ± 4.77	92.12 ± 2.77	92.11 ± 2.87
FC (Log CFU/100mL)	5.83 ± 0.63	4.25 ± 0.54a	3.90 ± 0.87a	3.94 ± 0.68a	3.94 ± 0.68a
Re (Ulog)		1.59 ± 0.58	1.94 ± 0.57	1.90 ± 0.57	1.79 ± 0.67
Phase III					
pH	7.69 ± 0.29	7.13 ± 0.18a	7.14 ± 0.13a	7.07 ± 0.12a	7.17 ± 0.18a
EC (mS/cm)	3.20 ± 0.05	3.40 ± 0.08a	3.80 ± 0.44a	3.84 ± 0.27a	3.83 ± 0.44a
DO (mg/L)	1.23 ± 1.21	1.03 ± 0.38a	1.68 ± 0.17b	1.68 ± 0.32b	1.54 ± 0.16b
Temperature (°C)	16.23 ± 2.68	14.48 ± 1.60a	14.28 ± 1.40a	14.52 ± 1.37a	14.32 ± 1.33a
COD (mg/L)	230.41 ± 41.34	90.20 ± 22.54a	66.29 ± 16.67ab	60.53 ± 19.27b	58.41 ± 16.86b
Re (%)		61.00 ± 5.02	71.35 ± 3.80	73.95 ± 4.66	74.81 ± 4.32
TSS (mg/L)	79.75 ± 25.42	18.38 ± 5.78a	8.25 ± 3.54b	11.00 ± 4.00b	9.13 ± 4.91b
Re (%)		73.12 ± 10.54	88.63 ± 3.82	83.50 ± 7.96	87.24 ± 6.41
TN (mg/L)	67.91 ± 9.73	54.88 ± 5.46a	26.00 ± 12.01b	11.16 ± 6.64c	21.48 ± 6.84bc
Re (%)		17.84 ± 14.78	58.62 ± 24.16	82.76 ± 10.40	67.89 ± 10.03
TP (mg/L)	5.83 ±0.61	4.39 ± 1.13a	1.40 ± 0.25b	0.66 ± 0.24b	2.68 ± 0.31c
Re (%)		25.18 ± 15.12	75.90 ± 3.92	88.64 ± 3.90	53.82 ± 5.31
Cu (mg/L)	2.04 ± 0.93	0.39 ± 0.12a	0.32 ± 0.11a	0.26 ± 0.08a	0.22 ± 0.12a
Re (%)		85.05 ± 6.10	88.73 ± 3.42	89.31 ± 4.72	95.29 ± 2.83
Cd (mg/L)	0.85 ± 0.37	0.19 ± 0.14a	0.09 ± 0.05a	0.12 ± 0.06a	0.08 ± 0.03a
Re (%)		78.20 ± 8.04	88.57 ± 3.56	85.32 ± 4.57	89.82 ± 2.50
FC (Log CFU/100mL)	5.75 ± 0.33	4.19 ± 0.69a	3.87 ± 0.42a	3.93 ± 0.65a	3.62 ± 0.65a
Re (Ulog)		1.56 ± 0.46	1.88 ± 0.33	1.82 ± 0.73	2.13 ± 0.21

Different superscript letters (a, b and c) indicate significantly different values (ANOVA, $p < 0.05$).

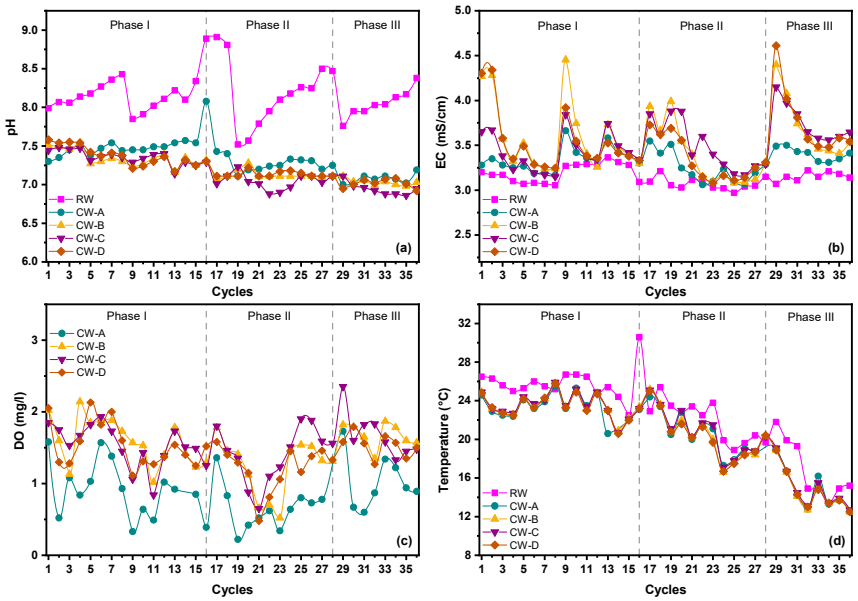

 doi:10.20944/preprints202604.2002.v1

Figure 3. Influent and effluent profiles of (a) pH, (b) EC, (c) DO and (d) temperature during the three experimental phases: Phase I (HRT = 24h), Phase II (HRT = 48h), and Phase III (HRT = 72h).

3.3. Organic Matters and Total Suspended Solids Removal

Chemical Oxygen Demand

The removal of organic matter in the four AVFCW mesocosms was evaluated through the monitoring of COD concentrations over the three operational phases. Figure 4-a and Table 2 shows COD mean concentration values in the systems during the experimental period. The average COD concentrations in the influent ranged between 230.41 ± 41.34 mg/L and 294.29 ± 80.44 mg/L, suggesting a relatively medium organic load in the raw wastewater [20]. During phase I, CW-A (control system) resulted in the highest effluent COD concentration (135.56 ± 25.65 mg/L), indicating the lowest organic matter removal. On the other hand, CW-B, CW-C and CW-D achieved improved performances, with average effluent COD concentrations of 72.20 ± 19.28 mg/L, 81.69 ± 26.76 mg/L, and 64.03 ± 18.15 mg/L, respectively. This trend was consistent through the subsequent phases. Statistical analysis revealed a significant difference between CW-A (the control system) and the AVFCWs amended with reactive media ($p < 0.05$). However, no significant differences were observed among CW-B, CW-C, and CW-D, although CW-D consistently outperformed all the systems.

Figure 5-a shows the COD removal efficiencies at different retention times (24 h, 48 h, and 72 h). At 24 h HRT (Phase I), Removal efficiencies of 72.90 ± 8.86%, 69.72 ± 7.80%, 65.32 ± 13.16% and 43.18 ± 11.27% were achieved in CW-D, CW-B, CW-C and CW-A, respectively. With the extension of HRT to 72 h (Phase III), the removal efficiencies of COD improved and become more stable in all AVFCW mesocosms, reaching 74.81 ± 4.32%, 73.95 ± 4.66%, 71.35 ± 3.80%, 61.00 ± 5.02% for CW-D, CW- C, CW-B and CW-A, respectively.

Total suspended solids

During the experiment, TSS concentrations in the raw wastewater were relatively low, as illustrated in Figure 4-b. This can be attributed to the use of primarily decanted wastewater, which was stored in a tank before being fed to the AVFCW mesocosms. The storage likely allowed additional settling, further reducing the TSS content. The average influent TSS concentrations were 73.69 ± 15.79 mg/L in Phase I, 72.83 ± 31.27 mg/L in Phase II, and 79.75 ± 25.42 mg/L in Phase III. The results show that the use of reactive media (pozzolan, clay, biochar, and mining residues) significantly ($p < 0.05$) improved TSS removal compared to the control system (CW-A). In CW-B, CW-C, and CW-D, the effluent TSS concentrations decreased to below 10 mg/L, with removal efficiencies exceeding 84% across all phases. In contrast, the TSS effluent concentration in CW-A was around 20 mg/L, corresponding to a removal efficiency of approximately 70%, as shown in Figure 5-b.

3.4. Nutrient Removal

Total Nitrogen

The TN concentrations in influent and effluents of the four AVFCWs across the different phases are shown in Figure 4-c and Table 2. The average influent concentration fluctuated between 88.06 ± 8.06 mg/L in phase I and 67.91 ± 9.73 mg/L in phase III. The TN effluent concentration of AVFCW mesocosms enriched with reactive media decreased significantly ($p < 0.05$) compared to the control system (CW-A), reaching 40.02 ± 16.41 mg/L for CW-D, 42.50 ± 15.14 mg/L for CW-C, and 47.92 ± 17.12 mg/L for CW-B, in contrast with 76.70 ± 12.60 mg/L for CW-A in Phase I. The same trend was observed in the subsequent phases, except for CW-C, which showed the highest removal, reaching a concentration of 11.16 ± 6.64 mg/L in phase III. The performance of CW-A remained consistently low throughout the experiment, despite a slight improvement with increased HRT. As presented in Figure 5-c, TN removal efficiencies of CW-A were 13.4 ± 7.81%, 19.3 ± 8.34%, and 17.8 ± 14.78% in Phases I, II, and III, respectively. On the other hand, CW-C achieved the highest TN removal efficiency in Phase III, at 82.8 ± 10.40%, followed by CW-D at 67.9 ± 10.03%, and CW-B at 58.6 ± 24.16%.

 doi:10.20944/preprints202604.2002.v1

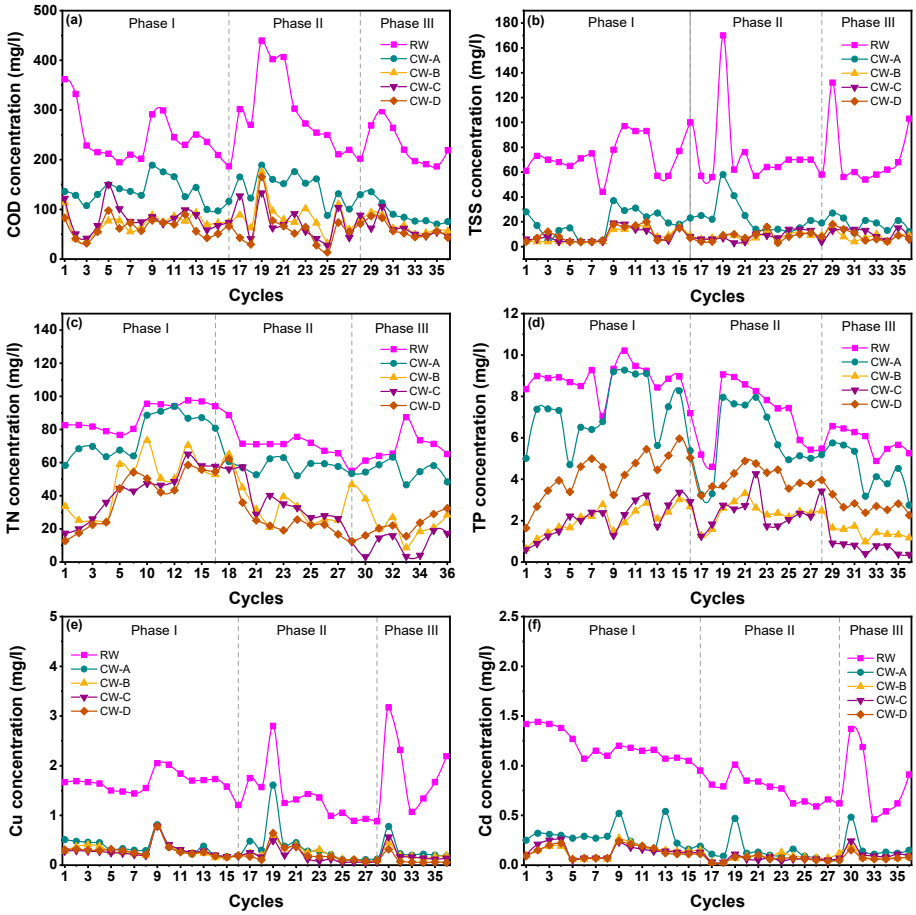

Figure 4. Influent and effluent profiles of (a) COD, (b) TSS, (c) TN, (d) TP, (e) Cu, and (f) Cd during the three experimental phases: Phase I (HRT = 24 h), Phase II (HRT = 48 h), and Phase III (HRT = 72 h).

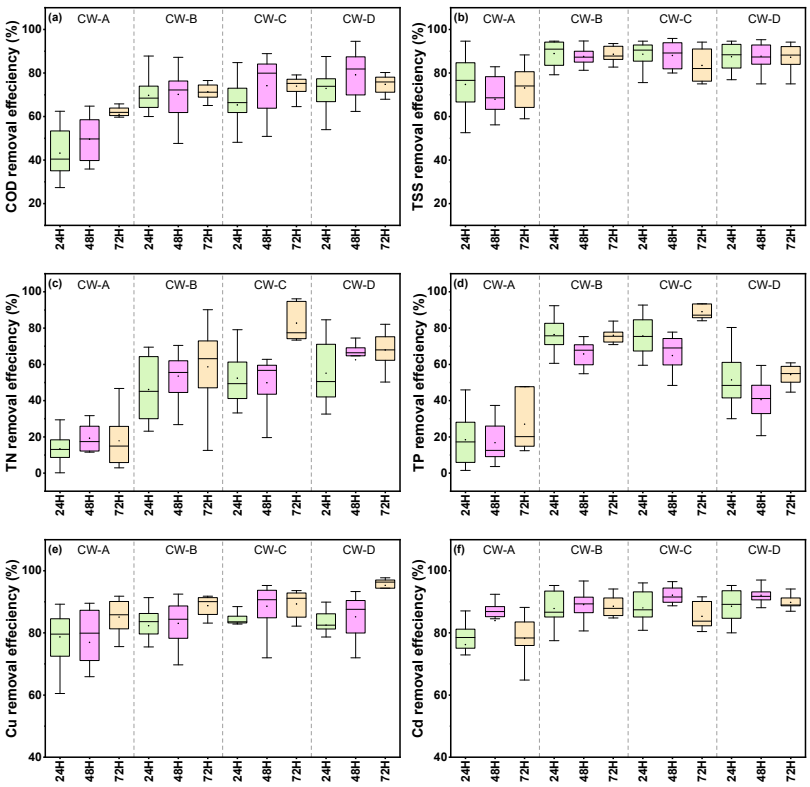

 doi:10.20944/preprints202604.2002.v1

Figure 5. Removal efficiency of (a) COD and (b) TSS (c) TN (d) TP (e) Cu (f) Cd at different HRTs (24 h, 48 h and 72 h).

Total phosphorus

The variations in TP concentrations between influent and effluent throughout the experiment are presented in Figure 4-d. The mean influent concentrations ranged between 8.77 ± 0.79 mg/L and 5.83 ± 0.61 mg/L within phases I and III, respectively as presented in Table 2. Through the experiment, CW-B and CW-C achieved the lowest concentration of TP, while CW-D showed moderate performance, with CW-A being the least effective. In phase I, CW-B and CW-C decreased the mean TP concentrations to 2.04 ± 0.67 mg/L and 2.11 ± 0.84 mg/L, respectively, compared to and 4.22 ± 1.11 mg/L for CW-D and 7.18 ± 1.52 mg/L for CW-A. The ANOVA test indicated that reactive media significantly influences TP removal. Indeed, CW-A had a statistically significant difference ($p < 0.05$) compared to the other AVFCWs. CW-B and CW-C significantly outperformed CW-D ($p < 0.05$) but did not differ from one another. Similar trends were observed in the subsequent phases. Figure 5-d shows the TP removal efficiency at different retention times. CW-B and CW-C achieved the highest removal efficiencies during phase I (76.41 ± 8.87% and 75.69 ± 10.11%, respectively), while CW-D showed moderate removal (51.41 ± 3.52%) and CW-A exhibited the lowest removal rate (18.40 ± 14.07%). However, prolonging the HRT to 72 h in Phase III further enhanced TP removal efficiencies, reaching 88.64 ± 3.90%, 75.90 ± 3.92%, 53.82 ± 5.31%, and 25.2 ± 15.12% for CW-C, CW-B, CW-D and CW-A, respectively.

3.5. Heavy Metals Removal

As presented in Table 2, the average influent concentrations of Cu and Cd ranged, across the three phases, from 2.04 ± 0.93 mg/L to 1.22 ± 0.29 mg/L and from 1.19 ± 0.15 mg/L to 0.75 ± 0.12 mg/L, respectively. Following the treatment, CW-A consistently exhibited the highest effluent concentrations of Cu and Cd, with considerable fluctuation throughout the experiment as shown in Figure 4-e, f. However, there was no statistically significant difference compared to the other AVFCWs. CW-B, CW-C, and CW-D maintained average effluent Cu concentrations below 0.3 mg/L, meeting the Moroccan irrigation standard, while their average Cd concentrations ranged from 0.19 mg/L to 0.06 mg/L, exceeding the allowable limit of 0.03 mg/L.

As shown in Figure 5-e, f, increasing HRT generally improved the removal of Cu and Cd. At an HRT of 72 h, the maximum Cu removal efficiencies were 95.29 ± 2.83%, 89.31 ± 4.72%, 88.73 ± 3.42% and 85.05 ± 6.10% for CW-D, CW-C, CW-B and CW-A respectively, while the lowest removal rates were observed at an HRT of 24 h. Moreover, longer HRT reduced variability, leading to a more consistent performance. The highest removal rates for Cd were observed at 48 h, reaching 92.12 ± 2.77%, 92.11 ± 2.87%, 89.08 ± 4.77%, and 83.93 ± 10.63% for CW-C, CW-D, CW-B and CW-A, respectively.

3.6. Faecal Coliforms Removal

The performance of the AVFCW mesocosms in removing faecal coliforms (FC) at different hydraulic retention times (HRTs) was monitored and presented in Figure 6. The mean influent FC concentrations varied slightly and were 4.90 ± 0.96 log CFU/100 mL in phase I, 5.83 ± 0.63 log CFU/100 mL in phase II, and 5.75 ± 0.33 log CFU/100 mL in phase III. During Phase I, CW-B, CW-C, and CW-D exhibited the highest removal efficiencies, achieving effluent concentrations of 1.78 ± 1.44, 1.97 ± 1.53, and 1.48 ± 1.48 log CFU/100 mL, respectively. This corresponds to log reductions of 3.08 ± 1.69 for CW-B, 2.92 ± 1.62 for CW-C and 3.42 ± 1.44 for CW-D. In contrast, CW-A showed the lowest removal efficiency of 1.27 ± 1.11, with a statistically significant difference ($p < 0.05$) compared to the other AVFCW mesocosms. However, during phases II and III, FC removal efficiencies of all AVFCW mesocosms decreased significantly, achieving comparable performance across the systems. The removal rates ranged from 1.59 ± 0.58 to 1.94 ± 0.57 log CFU/100 mL, in phase II and from 1.56 ± 0.46 to 2.13 ± 0.21 log CFU/100 mL in phase III.

 doi:10.20944/preprints202604.2002.v1

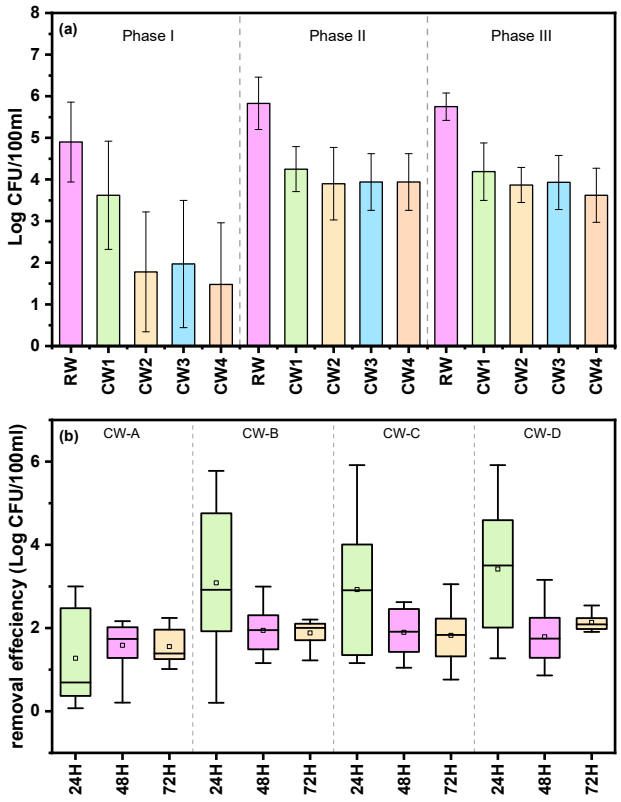

Figure 6. (a) Influent and effluent FC concentrations (b) FC removal efficiency across the three phases.

3.7. Principal Components Analysis and Correlation Matrix

Principal component analysis (PCA) was performed to identify underlying patterns and inter-relationships across 12 operational and effluent quality parameters. The first two principal components (PCs) captured a considerable proportion of the total variance (61.8%), accounting for 37.6% and 24.2%, respectively. PC3 supported a further 11.9%, increasing the cumulative variance to 73.7%. PC1 reveals a strong positive association between pH, temperature, COD, TSS, TN, TP and heavy metals, and a negative association with HRT and DO. Figure 7-a illustrates the distribution of the observations according to the HRT. It reveals a clear gradient across treatment phases, with Phase I (HRT = 24 h) characterized by higher contaminant loads, while Phases II and III (HRT = 48 h and 72 h, respectively) exhibit progressively lower concentrations of pollutants and increased dissolved oxygen levels. PC2, On the other hand, separates systems according to the physicochemical conditions and predominant treatment mechanisms. It exhibits strong positive loading on DO, pH, EC and temperature, in contrast with HRT, TSS, TN, TP and Log FC. The PCA biplot by system illustrated in Figure 7-b shows clearly differentiate CW-A from the three amended AVFCWs. CW-A is characterized by lower overall performance. In contrast, CW-B, CW-C, and CW-D partially overlap in the negative to neutral PC2 and lower PC1 indicating similar overall performance.

Figure 8 illustrates spearman correlation. Spearman correlation showed positive correlations between COD and TSS, TN and TP (up to r = 0.53), with a strong relationship between TN and TP (r = 0.62). Heavy metals were strongly associated (r = 0.61) and moderately correlated with COD and TSS and pH. Faecal coliforms, on the other hand, showed a positive correlation with TSS (r = 0.42) and a negative association with temperature (r = 0.44.

 doi:10.20944/preprints202604.2002.v1

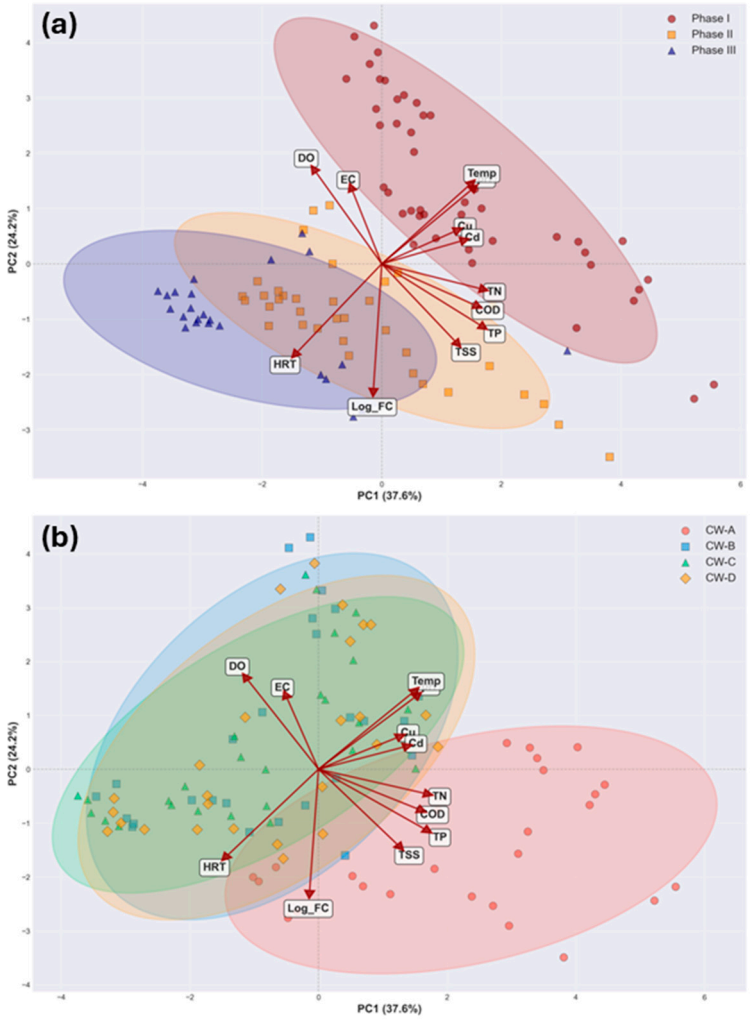

Figure 7. Multivariate analysis of AVFCWs performance: (a) PCA biplot showing sample distribution according to operational phase (b) PCA biplot illustrating sample distribution according to system configuration.

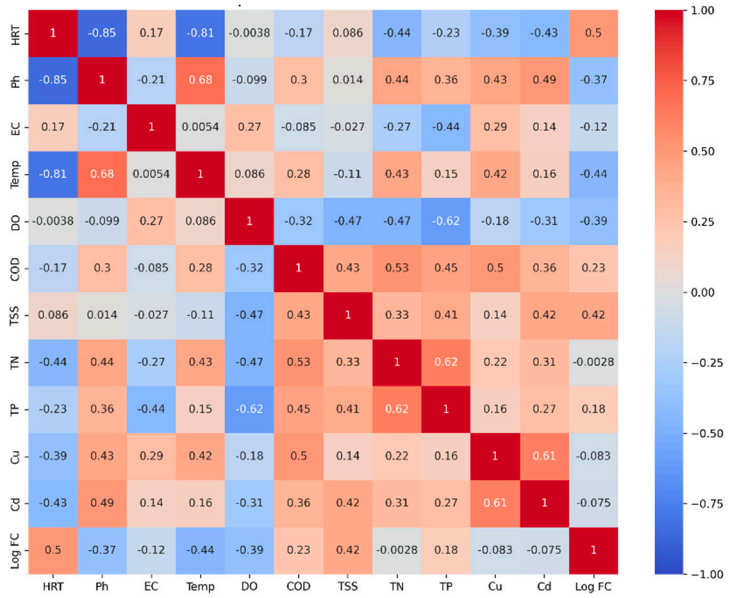

Figure 8. Spearman correlation matrix between operational and effluent quality parameters.

 doi:10.20944/preprints202604.2002.v1

3.8. Evapotranspiration and Water Loss in Constructed Wetlands

The evapotranspiration (ET) and corresponding water loss rates in the AVFCWs were assessed through the three phases and presented in Table 3. During phase I, ET ranged between 13.11 ± 6.65 mm/day and 10.16 ± 6.19 mm/day, with CW-A having the lowest ET among all the AVFCWs. This phase was characterised by warmer temperatures, with an average of 24.01 °C, promoting higher rates of evapotranspiration. In the subsequent phases, ET decreased slightly in all systems, reflecting the seasonal decline in temperature, which dropped to 20.08 °C in phase II and 14.09 °C in phase III.

In phase I, water loss was moderate across the AVFCWs with an average of 6.78 ± 4.13%, 8.63 ± 5.81%, 8.74 ± 4.43% and 8.41 ± 6.92% for CW-A, CW-B, CW-C and CW-D, respectively. In phase III, the water loss increased considerably, especially for the amended systems, reaching 14.57 ± 3.08%, 24.81 ± 6.71%, 27.55 ± 6.04%, and 27.11 ± 7.13% for CW-A, CW-B, CW-C, and CW-D, respectively.

Table 3. Water loss in the constructed wetlands across the phases.

		ET (mm/day)	Water loss (%)
Phase I	**CW-A**	10,16 ± 6,19	6,78 ± 4,13
	CW-B	12,94 ± 8,71	8,63 ± 5,81
	CW-C	13,11 ± 6,65	8,74 ± 4,43
	CW-D	12,62 ± 10,37	8,41 ± 6,92
Phase II	**CW-A**	5,14 ± 2,43	7,20 ± 3,40
	CW-B	10,04 ± 3,83	14,06 ± 5,36
	CW-C	12,15 ± 3,90	17,01 ± 5,45
	CW-D	13,17 ± 4,25	18,44 ± 5,95
Phase III	**CW-A**	6,94 ± 1,47	14,57 ± 3,08
	CW-B	11,81 ± 3,20	24,81 ± 6,71
	CW-C	13,12 ± 2,88	27,55 ± 6,04
	CW-D	12,91 ± 3,39	27,11 ± 7,13

4. Discussion

The present study demonstrated that both substrate type and hydraulic retention time governed the AVFCWs performance, with phosphate mining residues exhibiting high potential as substrate for constructed wetlands. Overall, the amended AVFCWs mesocosms consistently outperformed the sand-based system across all monitored parameters. This improvement is mainly related to the distinct physicochemical properties of the materials, as evidenced by their characterization. The porous structure and the high specific surface area of biochar, the mineral composition of phosphate mining residues and clay (notably the presence of P, Ca, Al, and Fe), and the alkaline character of all materials provided more favorable conditions for pollutant retention and transformation.

The environmental conditions established within the AVFCW mesocosms beds provided insight into the underlying treatment processes. The effluent pH was reduced and stabilized to near neutral in all systems, mainly driven by active biochemical processes. In fact, organic matter biodegradation produces carbon dioxide (CO_2) under aerobic conditions and organic acids in anaerobic zones [21,22] while nitrification releases H^+ neutralizing hydroxyl ions [23,24]. Moreover, the hydraulic retention time increasing from phase I to phase III may have further lowered the pH due to prolonged nitrification, organic matter decomposition and CO_2 accumulation. Meanwhile, a slight increase in EC was observed in the amended systems, likely due to organic matter mineralization releasing inorganic ions such as sulphates, phosphates, nitrates, etc. and increasing total dissolved solids in wastewater. This rise may also reflect ions concentration by evapotranspiration [25] and ions (e.g. Na^+, K^+, Mg^{2+}, and Ca^{2+}) release from the substrates through dissolution or ions exchange [9,26]. DO levels increased significantly in CW-B, CW-C, and CW-D, which could be due to the porous substrates, namely pozzolan and biochar, which enlarge the surface area for microbial activity and improve oxygen transfer within the wetlands bed [27]. Nevertheless, DO levels in all systems

 doi:10.20944/preprints202604.2002.v1

remained consistently below the 2.0 mg/L limit, recognized as the threshold for aerobic conditions, indicating that the AVFCWs operated predominantly under anoxic conditions, thereby limiting nitrification and hindering oxygen-dependent microbial processes. In addition, temperature likely played an important role in the system performance. The gradual temperature decline across the phases (from 24.01 °C to 14.09 °C), reflecting seasonal variation, may have further influenced microbial activity, oxygen solubility and consequently the overall treatment performances. A temperature of 15 °C is generally considered as a threshold below which bacterial activity and plant growth are significantly hindered [28,29]. In this study, phase III, during which the temperature dropped below 15 °C, coincided with an extended HRT (72 h), which may have mitigated the unfavorable effects of low temperature on treatment efficiency.

The enhanced COD removal in the AVFCW mesocosms, compared to CW-A, may be attributed to the combined effect of reactive media and the favorable environmental conditions, with CW-D consistently outperforming all the systems. These results align with previous studies emphasizing the beneficial effects of using reactive media in constructed wetlands [9,30,31]. The porous structure of the materials, observed on SEM images together with the relatively high specific surface area confirmed by BET measurements, provide an increased surface area for microbial attachment and enhance oxygen transfer within the beds, thereby improving organic matter biodegradation [32–34]. The lower COD removal efficiencies achieved in this study compared to some previous studies [8,35] could be attributed to the presence of heavy metals in the wastewater, which form stable complexes with organic matter. These complexes are less susceptible to microbial degradation [14,36]. Furthermore, COD removal efficiencies improved from phase I to phase III demonstrating that longer HRT allows for an extended contact time between pollutants and active biofilms, leading to enhanced microbial degradation of organic matter and reduced variability within the systems [37,38]. However, the temperature decline may have partially counteracted this effect, and the observed results likely reflect the confounding effect of both parameters. In contrast, removal mechanisms of TSS differ from those governing organic matter removal, as they are mainly driven by physical processes, including sedimentation, filtration, and interception by microbial biofilms [8,22]. Several factors influence these processes, including plant root density, feeding mode, substrate type and HRT. In the present study, CW-B, CW-C and CW-D consistently outperformed CW-A in TSS removal. These findings support previous studies indicating that reactive or fine media enhances TSS removal by increasing the available surface area for filtration and biofilm development [39,40]. Although previous studies have demonstrated that longer HRT improves TSS removal efficiency [38,41], extending the HRT from 24 to 72 h had no significant effect on TSS removal in this study.

Nitrogen removal in CWs is a complex process primarily attributed to ammonia volatilization, nitrification, denitrification, plant uptake, and substrate adsorption [22,42,43]. In the present study, TN removal improved significantly with increasing HRT across all the AVFCW mesocosms, although seasonal variation between the phases may have modulated microbial removal rates. The performance of CW-A remained consistently low throughout the experiment, despite a slight improvement with increased HRT, due to the limited porosity and oxygen transfer of the sand bed, which constrained the establishment of nitrifying microbial communities. On the other hand, CW-C achieved the highest TN removal efficiency in phase III, followed by CW-D and CW-B. The functional properties of the reactive media supported TN removal mechanisms. Clay and mining residues offer high cation exchange capacity for NH_4^+, which likely explains the high nitrogen removal observed in CW-C and CW-B under longer HRT. This is evidenced by the presence of abundant K^+ in illitic clay and Ca^{2+} in mining residues, as confirmed by EDS analysis. Moreover, biochar may provide a carbon source for denitrifying bacteria through the gradual release of dissolved organic matter, while enhancing electron transfer [32,33]. The porous structure and high surface area of all reactive media further support nitrification and denitrification by enhancing oxygen transfer and microbial development [44].

Total phosphorus is removed through the combined action of biotic processes, such as plant uptake and microbial immobilization, and abiotic mechanisms, including adsorption, precipitation,

 doi:10.20944/preprints202604.2002.v1

and complexation [45,46], with removal efficiency largely governed by substrate type and HRT [32,47]. Throughout the experiment, CW-B and CW-C achieved the lowest effluent TP concentrations, while CW-D exhibited moderate performance, with CW-A being the least effective. These results emphasize the crucial role of substrates in phosphorus removal. Mineral based materials promoted phosphorus removal by providing strong binding sites for adsorption and precipitation. Indeed, XRD and EDS analyses confirmed the presence of calcium-rich fluorapatite phosphate mining residues, enabling Ca-P precipitation [11,12,48]. Illite clay provided abundant Al/Fe-OH sites for phosphorus adsorption through ligand exchange and complexation [49–51]. On the other hand, the AVFCW mesocosm packed with raw biochar achieved moderate TP removal due to its negatively charged surface [52,53].

Heavy metals represent a significant concern for human health and the environment. Their removal from treated wastewater intended for agricultural reuse is therefore of paramount importance. In constructed wetlands, both biotic processes (mainly plant uptake) and abiotic processes including adsorption, precipitation, and complexation, contribute to heavy metal removal. Following treatment, all systems achieved high Cu and Cd removal efficiencies, with CW-A consistently exhibiting the highest effluent concentrations, with considerable fluctuation throughout the experiment. This highlights the contribution of plant uptake and suspended solids filtration to heavy metal removal [54,55]. Furthermore, plants promote the transformation of metals by inducing chemical changes in the rhizosphere through oxygen transport, organic carbon release, and sulfur cycling [56]. However, in this study, biotic processes were insufficient to meet the stringent requirements for agricultural reuse for Cd concentrations. In contrast, CW-B, CW-C, and CW-D maintained average effluent Cu concentrations below 0.3 mg/L, meeting the Moroccan irrigation standard. The enhanced heavy metal removal observed in the AVFCW mesocosms is likely attributed to the physicochemical properties of the reactive media. Inorganic anions released within the system can form complexes and precipitates with heavy metal ions, thereby reducing effluent concentration [14]. The alkaline character of the reactive media (pH = 8.1–8.75) further supports the formation of metal carbonates and metal hydroxides, among other precipitates, governed by pH and the availability of key anions (e.g., HCO_3^-, CO_3^{2-} and OH^-) [13]. The presence of biochar across all amended AVFCW mesocosms may have further improved heavy metal adsorption, owing to its relatively high specific area (366.15 m^2/g) and abundant functional groups and exchangeable ions as previously reported in several studies [14,36,57]. Mining residues, on the other hand, promote heavy metal immobilization through Ca/P precipitation, attributable to their high Ca (25.35%) and P content (7.79%), as well as surface adsorption through electrostatic interactions [58,59]. Illite clay leverages heavy metal removal through its cation exchange capacity, along with Al-OH/Fe-OH surface complexation [60,61]. Finally, increasing HRT generally enhanced Cd and Cu removal and reduced effluent variability, leading to a more stable and consistent performance.

The removal of pathogens in constructed wetlands involves several physical, chemical and biological processes. Physical mechanisms, including adsorption, filtration, and sedimentation, play a significant role in the initial retention of pathogens. Chemical factors include oxidation, solar radiation, and biocide excreted by roots. Biological processes consist of predation by protozoa, competition with native microbial communities, and natural die-off under adverse environmental conditions [62,63]. The effectiveness of these processes is considerably influenced by environmental factors such as temperature, solar radiation, dissolved oxygen availability, and hydraulic retention time [64,65]. In this study, the microbiological results revealed the main limitation of the system. Although the amended AVFCW mesocosms achieved up to 3-log FC reduction during phase I, the removal efficiency decreased significantly in the subsequent phases, with all systems reaching similarly moderate performances. This decrease could be attributed to lower temperatures, as higher FC removal rates are typically achieved during warmer summer months [66,67]. Extended retention times stabilized the removal efficiencies rather than enhanced them, which disagrees with previous studies [66]. This suggests that the confounding temperature decline masked any positive HRT effect. Water losses at longer HRT may also have concentrated FC in the effluent. The impact of reactive

 doi:10.20944/preprints202604.2002.v1

media was not significant which is inconsistent with previous studies demonstrating that reactive media, especially biochar, enhance pathogen removal [68]. Accordingly, the concentration of FC exceeded the limit for wastewater reuse in agriculture in Morocco, set at 1000 CFU/100 mL indicating that single-stage AVFCWs are not sufficient for pathogen removal. Thus, the integration of additional polishing steps such as a second CW stage, ultraviolet (UV) disinfection or chlorination is required.

PCA and Spearman correlation analyses offer a comprehensive overview of pollutant removal mechanisms in the AVFCW mesocosms, elucidating performance differences across treatment phases and wetland configurations. PC1 revealed a strong positive association between pH, temperature, COD, TSS, TN, TP and heavy metals, and a negative association with HRT and DO, suggesting that increases in one parameter were generally accompanied by increases in others. Notably, PC1 also reflected a gradient driven by the combined effect of increasing HRT and declining temperature, reflecting a confounding interaction between these two variables. The distribution of the observations according to the HRT revealed a clear gradient across treatment phases, with Phase I (HRT = 24 h) characterized by higher contaminant loads, while Phases II and III (HRT = 48 h and 72 h, respectively) exhibiting progressively lower pollutant concentrations and increased dissolved oxygen levels, emphasizing the significant influence of HRT on treatment performance. At the same time, this gradient reflected seasonal variability, marked by declining temperatures across the phases, which likely influenced microbial activity. On the other hand, PC2 separated systems according to prevailing physicochemical conditions and predominant treatment mechanisms, with strong positive loadings on DO, pH, EC and temperature, in contrast with HRT, TSS, TN, TP and Log FC. Positive PC2 suggested enhanced aerobic biodegradation and nitrification, while negative scores reflected higher contributions from denitrification, adsorption, precipitation and filtration. The system based biplot reinforced the mechanistic contributions of reactive media with CW-A distinctly separated from the amended AVFCW mesocosms, confirming its limited treatment capacity and the predominance of biological processes. In contrast, CW-B, CW-C, and CW-D partially overlaped in the negative to neutral PC2 region and lower PC1 scores, indicating comparable overall performance. This confirms that reactive media enhanced treatment efficiency through combined biological and physicochemical mechanisms. Notably, CW-C and CW-B consistently occupied regions with lower TN and TP, consistent with their higher nutrient removals. This finding highlighted the capacity of mining residues and clay to promote ion exchange, adsorption, precipitation, and surface complexation alongside biological transformation.

Spearman correlations supported and complemented PCA results, providing a consistent representation of pollutant removal in the AVFCWs. Positive correlations between COD and TSS, TN and TP, along with their loading in the same direction on PC1 in opposition to HRT and DO, indicated that organic matter, suspended solids and nutrients were partially removed through coupled processus. These processus included filtration and precipitation, biodegradation, nitrification/denitrification, especially in well aerated zones. Heavy metals were strongly associated and moderately correlated with COD and TSS and pH, suggesting partial co-removal with organic and particulate matter, in addition to adsorption, precipitation and complexation on Ca, P, Al and Fe rich substrates, particularly in clay and mining residues. Faecal coliforms, on the other hand, exhibited a positive correlation with TSS and a negative association with temperature, indicating that FC are partially eliminated with particular matter with reduced inactivation in low temperatures.

Water loss through evapotranspiration emerges as an important consideration for wastewater reuse, particularly in arid to semi-arid regions. Phase I recorded the highest ET rates (10.16 ± 6.19 – 13.11 ± 6.65 mm/day), coinciding with warmer temperatures (24.01 °C), with CW-A exhibiting the lowest ET among all systems. In the subsequent phases, ET decreased slightly in all systems, reflecting the seasonal decline in temperature, which dropped to 20.08 °C in phase II and 14.09 °C in phase III. These results are consistent with previous studies that reported ET rates for Arundo donax ranging between 5 and 40 mm/day [69–71]. Furthermore, the use of reactive media enhanced ET compared to sand-based systems, aligning with previous studies that indicate that substrates characterized by significant porosity and organic matter content tend to increase the ET due to their

 doi:10.20944/preprints202604.2002.v1

higher water retention capacity and enhanced plant growth [72,73]. The water loss followed a trend consistent with evapotranspiration but increased considerably with longer HRT, rising considerably from phase I to phase III, particularly in the amended systems. These results were consistent with reported water losses reaching 28% when using Arundo donax as a plant [71]. This increase is attributable to the prolonged interaction between water, plants, and substrates, enhancing both transpiration and surface evaporation [22,74]. Overall, these findings emphasize that substrate type and extended HRT may result in greater water losses, which could pose challenges for wastewater reuse by concentrating salts and reducing the treated wastewater volume. Consequently, careful media selection and HRT optimization are critical for balancing treatment performance with water conservation, especially in semi-arid to arid regions.

5. Conclusions

This mesocosm-scale study provided an evaluation of phosphate mining residues as a novel reactive substrate for constructed wetlands. The results demonstrated that the incorporation of reactive media significantly enhanced pollutant removal compared to sand based system. CW-D achieved the highest overall performance for COD and TSS removal, while CW-B and CW-C outperformed in phosphorus and heavy metal removal through adsorption, precipitation and cation exchange. Notably, phosphate mining residues achieved 76% phosphorus removal and up to 89% Cd and Cu removal, positioning them as a viable alternative to conventional substrates.

On the other hand, the treated wastewater did not meet the Moroccan agricultural reuse standards for cadmium and faecal coliforms. The Cd noncompliance is mainly attributable to the high challenge load applied in this study, whereas faecal coliform removal was limited in all systems, especially under low temperatures. These results suggest that single stage AVFCWs are insufficient and require additional polishing steps for safe agricultural reuse. Moreover, the subsequent phases with increasing HRT coincided with seasonal temperature decline, resulting in a combined influence of both factors that may have masked the positive individual effect of HRT on treatment performance. Extended HRT also increased water loss through ET, reaching up to 28%, thereby reducing the available treated wastewater volume for reuse.

These findings were obtained under greenhouse conditions at mesocosm scale. Further validation is necessary for extrapolating to field-scale systems, including: (i) used substrate characterization and microbial community analysis to elucidate treatment mechanisms; (ii) Optimization of operational parameters (e.g. hydraulic loading rate, bed depth, reactive media ratios, etc.); (iii) Long-term performance monitoring to evaluate substrate ageing and saturation; (iv) Integration of additional treatment steps (two stage CWs) to achieve regulatory compliance; (v) pilot-scale trials with economic and environmental assessment to evaluate feasibility for decentralized wastewater treatment in rural Morocco.

Supplementary Materials: The following supporting information can be downloaded at the website of this paper posted on Preprints.org, Figure S1. SEM images and corresponding EDS spectra of (a) phosphate mining residues (b) Clay (c) Pozzolan and (d) Biochar.

Author Contributions: Conceptualization, M.H.,M.C.N., J.L. and N.R.; methodology, M.H; software, M.H.; validation, M.H., M.C.N., J.L., A.A., B.G. and N.R.; formal analysis, M.H.; investigation, M.H.; resources, M.C.N., A.A., B.G., N.R.; data curation, M.H.; writing—original draft preparation, M.H.; writing—review and editing, M.H., M.C.N., J.L., A.A., B.G. and N.R.; visualization, M.H.; supervision, M.C.N., J.L., N.R.; project administration, M.H., M.C.N., N.R.; funding acquisition, M.C.N., N.R. All authors have read and agreed to the published version of the manuscript.

Funding: This research received no external funding.

Data Availability Statement: The original contributions presented in this study are included in the article. Further inquiries can be directed to the corresponding authors.

 doi:10.20944/preprints202604.2002.v1

Acknowledgments: This research was financially supported by Mohammed VI Polytechnic University (UM6P). The authors gratefully acknowledge the technical support provided by the staff of the experimental farm of Mohammed VI Polytechnic University (UM6P) and the personnel at the Benguerir Wastewater Treatment Plant. We would also thank Younes El Haimer, Mohammed El Ajoumi, and Yassine Jari for their assistance with sampling and laboratory work.

Conflicts of Interest: The authors declare no conflicts of interest.

References

1. UNESCO The United Nations World Water Development Report 2023 Partnerships and Cooperation for Water; 2023;
2. FAO The State of the World's Land and Water Resources for Food and Agriculture 2021 – Systems at Breaking Point; 2022; ISBN 9789251361276.
3. Lahlou, F.Z.; Mackey, H.R.; Al-Ansari, T. Wastewater Reuse for Livestock Feed Irrigation as a Sustainable Practice: A Socio-Environmental-Economic Review. *J. Clean. Prod.* **2021**, *294*, 126331, doi:10.1016/j.jclepro.2021.126331.
4. Ofori, S.; Puškáčová, A.; Růžičková, I.; Wanner, J. Treated Wastewater Reuse for Irrigation: Pros and Cons. *Sci. Total Environ.* **2021**, *760*, doi:10.1016/j.scitotenv.2020.144026.
5. Zhang, X.; Dou, Y.; Gao, C.; He, C.; Gao, J.; Zhao, S.; Deng, L. Science of the Total Environment Removal of Cd (II) by Modi Fi Ed Maifanite Coated with Mg-Layered Double Hydroxides in Constructed Rapid in Fi Ltration Systems. **2019**, *685*, 951–962, doi:10.1016/j.scitotenv.2019.06.228.
6. Hdidou, M.; Necibi, M.C.; Labille, J.; Hajjaji, S. El; Dhiba, D.; Chechbouni, A.; Roche, N. Potential Use of Constructed Wetland Systems for Rural Sanitation and Wastewater Reuse in Agriculture in the Moroccan Context. *Energies* **2022**, *15*, doi:10.3390/en15010156.
7. Almuktar, S.A.A.A.N.; Abed, S.N.; Scholz, M. Wetlands for Wastewater Treatment and Subsequent Recycling of Treated Effluent: A Review. *Environ. Sci. Pollut. Res.* **2018**, *25*, 23595–23623, doi:10.1007/s11356-018-2629-3.
8. Kotsia, D.; Deligianni, A.; Fyllas, N.M.; Stasinakis, A.S.; Fountoulakis, M.S. Converting Treatment Wetlands into "Treatment Gardens": Use of Ornamental Plants for Greywater Treatment. *Sci. Total Environ.* **2020**, *744*, doi:10.1016/j.scitotenv.2020.140889.
9. Wang, Y.; Cai, Z.; Sheng, S.; Pan, F.; Chen, F.; Fu, J. Comprehensive Evaluation of Substrate Materials for Contaminants Removal in Constructed Wetlands. *Sci. Total Environ.* **2020**, *701*, 134736, doi:10.1016/j.scitotenv.2019.134736.
10. Chlahbi, S.; Belem, T.; Elghali, A.; Rochdane, S.; Zerouali, E.; Inabi, O.; Benzaazoua, M. Geological and Geomechanical Characterization of Phosphate Mine Waste Rock in View of Their Potential Civil Applications: A Case Study of the Benguerir Mine Site, Morocco. *Minerals* **2023**, *13*, doi:10.3390/min13101291.
11. Troesch, S.; Esser, D.; Molle, P. Natural Rock Phosphate: A Sustainable Solution for Phosphorous Removal from Wastewater. *Procedia Eng.* **2016**, *138*, 119–126, doi:10.1016/j.proeng.2016.02.069.
12. Molle, P.; Liénard, A.; Grasmick, A.; Iwema, A.; Kabbabi, A. Apatite as an Interesting Seed to Remove Phosphorus from Wastewater in Constructed Wetlands. *Water Sci. Technol.* **2005**, *51*, 193–203, doi:10.2166/wst.2005.0318.
13. Yu, G.; Li, P.; Wang, G.; Wang, J.; Zhang, Y.; Wang, S.; Yang, K. A Review on the Removal of Heavy Metals and Metalloids by Constructed Wetlands : Bibliometric , Removal Pathways , and Key Factors. *World J. Microbiol. Biotechnol.* **2021**, *37*, 1–12, doi:10.1007/s11274-021-03123-1.
14. Zhang, Y.; Dong, Y.; Qin, L.; Yue, X.; Zhou, A.; Wu, H. Distinct Roles of Biochar and Pyrite Substrates in Enhancing Nutrient and Heavy Metals Removal in Intermittent-Aerated Constructed Wetlands: Performances and Mechanism. *Environ. Res.* **2024**, *258*, 119393, doi:10.1016/j.envres.2024.119393.
15. Chen, F.; Sun, Y.; Liang, C.; Yang, T.; Mi, S.; Dai, Y.; Yu, M.; Yao, Q. Adsorption Characteristics and Mechanisms of Cd2+ from Aqueous Solution by Biochar Derived from Corn Stover. *Sci. Rep.* **2022**, *12*, 1–17, doi:10.1038/s41598-022-22714-y.

 doi:10.20944/preprints202604.2002.v1

16. Dotro, G.; Molle, P.; Nivala, J.; Puigagut, J.; Stein, O. *Biological Wastewater Treatment Series, Treatment Wetlands*; 2017; Vol. 7; ISBN 9781780408767.
17. Urumović, K. The Referential Grain Size and Effective Porosity in the Kozeny-Carman Model. *Hydrol. Earth Syst. Sci.* **2016**, *20*, 1669–1680, doi:10.5194/hess-20-1669-2016.
18. Liu, H.; Hu, Z.; Zhang, J.; Ngo, H.H.; Guo, W.; Liang, S.; Fan, J.; Lu, S.; Wu, H. Optimizations on Supply and Distribution of Dissolved Oxygen in Constructed Wetlands: A Review. *Bioresour. Technol.* **2016**, *214*, 797–805, doi:10.1016/j.biortech.2016.05.003.
19. Wang, S.; Teng, Y.; Cheng, F.; Lu, X. Application Potential of Constructed Wetlands on Different Operation Mode for Biologically Pre-Treatment of Rural Domestic Wastewater. *Sustain.* **2023**, *15*, doi:10.3390/su15031799.
20. Metcalf & Eddy Wastewater Engineering: Treatment and Resource Recovery. **2013**.
21. He, K.; Lv, T.; Wu, S.; Guo, L.; Ajmal, Z.; Luo, H.; Dong, R. Treatment of Alkaline Stripped Effluent in Aerated Constructed Wetlands: Feasibility Evaluation and Performance Enhancement. *Water (Switzerland)* **2016**, *8*, doi:10.3390/w8090386.
22. Kadlec, R.H.; Wallace, S. *Treatment Wetlands*; 2008; ISBN 9781566705264.
23. Amiri, K.; Bekkari, N. eddine; Debbakh, A.E.; Chaib, W.; Kherifi, W. Urban Wastewater Treatment by Pilot-Scale Vertical Subsurface Flow Constructed Wetland Planted with Typha Latifolia and Phragmite Australis Under Arid Climate. *Water. Air. Soil Pollut.* **2022**, *233*, doi:10.1007/s11270-022-05802-7.
24. Vymazal, J. Removal of Nutrients in Various Types of Constructed Wetlands. *Sci. Total Environ.* **2007**, *380*, 48–65, doi:10.1016/j.scitotenv.2006.09.014.
25. Singh, S.; Suman, S.K.; Dutta, K.; Daverey, A. Comparison of Canna Indica and Acorus Calamus for Surfactant Removal in Biochar Augmented Constructed Wetlands. *Environ. Chem. Ecotoxicol.* **2025**, *7*, 130–140, doi:10.1016/j.enceco.2024.11.003.
26. Sharma, R.; Malaviya, P. Enhanced Textile Wastewater Remediation in Phragmites Karka-Based Vertical Flow Constructed Wetlands Using Phragmites-Derived Biochar. *Chemosphere* **2024**, *366*, 143529, doi:10.1016/j.chemosphere.2024.143529.
27. Fu, G.; Wu, J.; Han, J.; Zhao, L.; Chan, G.; Leong, K. Effects of Substrate Type on Denitrification Efficiency and Microbial Community Structure in Constructed Wetlands. *Bioresour. Technol.* **2020**, *307*, doi:10.1016/j.biortech.2020.123222.
28. Gholipour, A.; Stefanakis, A.I. A Full-Scale Anaerobic Baffled Reactor and Hybrid Constructed Wetland for University Dormitory Wastewater Treatment and Reuse in an Arid and Warm Climate. *Ecol. Eng.* **2021**, *170*, 106360, doi:10.1016/j.ecoleng.2021.106360.
29. Udom, I.J.; Mbajiorgu, C.C.; Oboho, E.O. Development and Evaluation of a Constructed Pilot-Scale Horizontal Subsurface Flow Wetland Treating Piggery Wastewater. *Ain Shams Eng. J.* **2018**, *9*, 3179–3185, doi:10.1016/j.asej.2018.04.002.
30. Yang, Y.; Zhao, Y.; Liu, R.; Morgan, D. Global Development of Various Emerged Substrates Utilized in Constructed Wetlands. *Bioresour. Technol.* **2018**, *261*, 441–452, doi:10.1016/j.biortech.2018.03.085.
31. Yang, C.; Zhang, X.; Tang, Y.; Jiang, Y.; Xie, S.; Zhang, Y.; Qin, Y. Selection and Optimization of the Substrate in Constructed Wetland: A Review. *J. Water Process Eng.* **2022**, *49*, 103140, doi:10.1016/j.jwpe.2022.103140.
32. Liu, M.; Li, B.; Xue, Y.; Wang, H.; Yang, K. Constructed Wetland Using Corncob Charcoal Substrate: Pollutants Removal and Intensification. *Water Sci. Technol.* **2017**, *76*, 1300–1307, doi:10.2166/wst.2017.305.
33. Sun, Y.; Zhou, P.; Zhang, N.; Zhang, Z.; Guo, Q.; Chen, C.; Cui, L. Effects of Matrix Modification and Bacteria Amendment on the Treatment Efficiency of Municipal Tailwater Pollutants by Modified Vertical Flow Constructed Wetland. *J. Environ. Manage.* **2021**, *281*, 111920, doi:10.1016/j.jenvman.2020.111920.
34. Xu, G.; Li, Y.; Hou, W.; Wang, S.; Kong, F. Effects of Substrate Type on Enhancing Pollutant Removal Performance and Reducing Greenhouse Gas Emission in Vertical Subsurface Flow Constructed Wetland. *J. Environ. Manage.* **2021**, *280*, 111674, doi:10.1016/j.jenvman.2020.111674.
35. Stefanatou, A.; Lagkadas, M.; Petousi, I.; Schiza, S.; Stasinakis, A.S.; Fyllas, N.; Fountoulakis, M.S. Vertical Flow Constructed Wetlands as Green Facades and Gardens for On-Site Greywater Treatment in Buildings:

 doi:10.20944/preprints202604.2002.v1

Two-Year Mesocosm Study on Removal Performance. *Sci. Total Environ.* **2024**, *906*, 167362, doi:10.1016/j.scitotenv.2023.167362.

36. Feng, L.; Zhang, Y.; Yang, J.; Guo, Z.; Zhang, J.; Wu, H. Applying Biochar Coupled with Pyrite Substrates Simultaneously Enhanced Nutrient and Heavy Metal Removal in Constructed Wetland: Performance and Mechanism. *Chem. Eng. J.* **2024**, *488*, 150868, doi:10.1016/j.cej.2024.150868.
37. Herrera-Cárdenas, J.; Navarro, A.E.; Torres, E. Effects of Porous Media, Macrophyte Type and Hydraulic Retention Time on the Removal of Organic Load and Micropollutants in Constructed Wetlands. *J. Environ. Sci. Heal. - Part A Toxic/Hazardous Subst. Environ. Eng.* **2016**, *51*, 380–388, doi:10.1080/10934529.2015.1120512.
38. Minakshi, D.; Sharma, P.K.; Rani, A. Effect of Filter Media and Hydraulic Retention Time on the Performance of Vertical Constructed Wetland System Treating Dairy Farm Wastewater. *Environ. Eng. Res.* **2022**, *27*, 0–3, doi:10.4491/eer.2020.436.
39. Thomaidi, V.; Petousi, I.; Kotsia, D.; Kalogerakis, N.; Fountoulakis, M.S. Use of Green Roofs for Greywater Treatment: Role of Substrate, Depth, Plants, and Recirculation. *Sci. Total Environ.* **2022**, *807*, 151004, doi:10.1016/j.scitotenv.2021.151004.
40. De Rozari, P.; Greenway, M.; El Hanandeh, A. An Investigation into the Effectiveness of Sand Media Amended with Biochar to Remove BOD_5, Suspended Solids and Coliforms Using Wetland Mesocosms. *Water Sci. Technol.* **2015**, *71*, 1536–1544, doi:10.2166/wst.2015.120.
41. Andreo-Martínez, P.; García-Martínez, N.; Quesada-Medina, J.; Almela, L. Domestic Wastewaters Reuse Reclaimed by an Improved Horizontal Subsurface-Flow Constructed Wetland: A Case Study in the Southeast of Spain. *Bioresour. Technol.* **2017**, *233*, 236–246, doi:10.1016/j.biortech.2017.02.123.
42. Panghal, V.; Singh, A.; Arora, D.; Kumar, S. Biochar-Modified Constructed Wetlands Using Eclipta Alba as a Plant for Sustainable Rural Wastewater Treatment. *Environ. Sci. Pollut. Res.* **2024**, *31*, 17299–17310, doi:10.1007/s11356-024-32144-0.
43. Lu, S.; Zhang, X.; Wang, J.; Pei, L. Impacts of Different Media on Constructed Wetlands for Rural Household Sewage Treatment. *J. Clean. Prod.* **2016**, *127*, 325–330, doi:10.1016/j.jclepro.2016.03.166.
44. Nguyen, X.C.; Nguyen, D.D.; Tran, Q.B.; Nguyen, T.T.H.; Tran, T.K.A.; Tran, T.C.P.; Nguyen, T.H.G.; Tran, T.N.T.; La, D.D.; Chang, S.W.; et al. Two-Step System Consisting of Novel Vertical Flow and Free Water Surface Constructed Wetland for Effective Sewage Treatment and Reuse. *Bioresour. Technol.* **2020**, *306*, 123095, doi:10.1016/j.biortech.2020.123095.
45. Ballantine, D.J.; Tanner, C.C. Substrate and Filter Materials to Enhance Phosphorus Removal in Constructed Wetlands Treating Diffuse Farm Runoff: A Review. *New Zeal. J. Agric. Res.* **2010**, *53*, 71–95, doi:10.1080/00288231003685843.
46. Ran, N. New Developments in Constructed Wetland Technology and Substrate Applications for Phosphorus Removal – A Review. *Wetlands* **2025**, *45*, doi:10.1007/s13157-025-01936-6.
47. Xing, C.; Xu, X.; Xu, Z.; Wang, R.; Xu, L. Study on the Decontamination Effect of Biochar-Constructed Wetland under Different Hydraulic Conditions. *Water (Switzerland)* **2021**, *13*, doi:10.3390/w13070893.
48. Molle, P.; Harouiya, N.; Prost-Boucle, S.; Morlay, C.; Esser, D.; Martin, S.; Besnault, S. Déphosphatation Des Eaux Usées Par Filtres Plantés Garnis de Phosphorites : Recommandations Pour Le Développement de La Filière. **2012**, 1–48.
49. Li, G.; Wang, Z.; Liu, Y.; Chu, X.; Qi, Z.; Liang, Z.; Yang, F.; Hu, X. Study on the Adsorption Mechanism and Response Surface Optimization of Fluorine and Phosphorus by the Red Clay in Guizhou. *ACS Omega* **2025**, doi:10.1021/acsomega.4c11344.
50. Patyal, V.; Jaspal, D.; Khare, K. Evaluation of Composite Matrix in Constructed Wetland for Phosphorus Removal. *Bioresour. Technol. Reports* **2024**, *26*, 101870, doi:10.1016/j.biteb.2024.101870.
51. Zhen, Z.; Yang, Y.; Liu, Z.; Sun, H.; He, C. Porous Red Mud Ceramsite for Aquatic Phosphorus Removal: Application in Constructed Wetlands. *Environ. Pollut.* **2024**, *360*, 124688, doi:10.1016/j.envpol.2024.124688.
52. Shang, Z.; Wang, Y.; Wang, S.; Jin, F.; Hu, Z. Enhanced Phosphorus Removal of Constructed Wetland Modified with Novel Lanthanum-Ammonia-Modified Hydrothermal Biochar: Performance and Mechanism. *Chem. Eng. J.* **2022**, *449*, 137818, doi:10.1016/j.cej.2022.137818.

 doi:10.20944/preprints202604.2002.v1

53. El Barkaoui, S.; Mandi, L.; Aziz, F.; Del Bubba, M.; Ouazzani, N. A Critical Review on Using Biochar as Constructed Wetland Substrate: Characteristics, Feedstock, Design and Pollutants Removal Mechanisms. *Ecol. Eng.* **2023**, *190*, 106927, doi:10.1016/j.ecoleng.2023.106927.
54. Zhou, Y.; Gu, T.; Yi, W.; Zhang, T.; Zhang, Y. The Release Mechanism of Heavy Metals from Lab-Scale Vertical Flow Constructed Wetlands Treating Road Runoff. *Environ. Sci. Pollut. Res.* **2019**, *26*, 16588–16595, doi:10.1007/s11356-019-05097-y.
55. Kumari, M.; Tripathi, B.D. Efficiency of Phragmites Australis and Typha Latifolia for Heavy Metal Removal from Wastewater. *Ecotoxicol. Environ. Saf.* **2015**, *112*, 80–86, doi:10.1016/j.ecoenv.2014.10.034.
56. Yeh, T.Y. Removal of Metals in Constructed Wetlands: Review. *Pract. Period. Hazardous, Toxic, Radioact. Waste Manag.* **2008**, *12*, 96–101, doi:10.1061/(ASCE)1090-025X(2008)12:2(96).
57. Wang, G.; Yu, G.; Chi, T.; Li, Y.; Zhang, Y.; Wang, J.; Li, P.; Liu, J.; Yu, Z.; Wang, Q.; et al. Insights into the Enhanced Effect of Biochar on Cadmium Removal in Vertical Flow Constructed Wetlands. *J. Hazard. Mater.* **2023**, *443*, 130148, doi:10.1016/j.jhazmat.2022.130148.
58. CORAMI, A.; MIGNARDI, S.; FERRINI, V. Removal of Lead, Copper, Zinc and Cadmium from Water Using Phosphate Rock. *Acta Geol. Sin. - English Ed.* **2008**, *82*, 1223–1228, doi:10.1111/j.1755-6724.2008.tb00724.x.
59. Gao, S.; Kang, X.; Li, Y.; Yu, J.; Wang, H.; Pan, H.; Yang, Q.; Yang, Z.; Sun, Y.; Zhuge, Y.; et al. Treatment of Cadmium-Contaminated Water Systems Using Modified Phosphate Rock Powder: Contaminant Uptake, Adsorption Ability, and Mechanisms. *Water (Switzerland)* **2024**, *16*, doi:10.3390/w16060862.
60. Echeverría, J.C.; Churio, E.; Garrido, J.J. Retention Mechanisms of Cd on Illite. *Clays Clay Miner.* **2002**, *50*, 614–623, doi:10.1346/000986002320679341.
61. Turan, N.G.; Elevli, S.; Mesci, B. Adsorption of Copper and Zinc Ions on Illite: Determination of the Optimal Conditions by the Statistical Design of Experiments. *Appl. Clay Sci.* **2011**, *52*, 392–399, doi:10.1016/j.clay.2011.04.010.
62. Wu, S.; Carvalho, P.N.; Müller, J.A.; Manoj, V.R.; Dong, R. Sanitation in Constructed Wetlands: A Review on the Removal of Human Pathogens and Fecal Indicators. *Sci. Total Environ.* **2016**, *541*, 8–22, doi:10.1016/j.scitotenv.2015.09.047.
63. Kaushal, M.; Patil, M.D.; Wani, S.P. Potency of Constructed Wetlands for Deportation of Pathogens Index from Rural, Urban and Industrial Wastewater. *Int. J. Environ. Sci. Technol.* **2018**, *15*, 637–648, doi:10.1007/s13762-017-1423-y.
64. El Ghadraoui, A.; Ouazzani, N.; Ahmali, A.; El Mansour, T.E.H.; Aziz, F.; Hejjaj, A.; Del Bubba, M.; Mandi, L. Treatment of Olive Mill and Municipal Wastewater Mixture by Pilot Scale Vertical Flow Constructed Wetland. *Desalin. Water Treat.* **2020**, *198*, 126–139, doi:10.5004/dwt.2020.26009.
65. Shingare, R.P.; Thawale, P.R.; Raghunathan, K.; Mishra, A.; Kumar, S. Constructed Wetland for Wastewater Reuse: Role and Efficiency in Removing Enteric Pathogens. *J. Environ. Manage.* **2019**, *246*, 444–461, doi:10.1016/j.jenvman.2019.05.157.
66. Ramprasad, C.; Smith, C.S.; Memon, F.A.; Philip, L. Removal of Chemical and Microbial Contaminants from Greywater Using a Novel Constructed Wetland: GROW. *Ecol. Eng.* **2017**, *106*, 55–65, doi:10.1016/j.ecoleng.2017.05.022.
67. de Rozari, P.; Krisnayanti, D.S.; Refli; Yordanis, K. V.; Atie, M.R.R. The Use of Pumice Amended with Sand Media for Domestic Wastewater Treatment in Vertical Flow Constructed Wetlands Planted with Lemongrass (Cymbopogon Citratus). *Heliyon* **2021**, *7*, doi:10.1016/j.heliyon.2021.e07423.
68. Chand, N.; Suthar, S.; Kumar, K.; Tyagi, V.K. Enhanced Removal of Nutrients and Coliforms from Domestic Wastewater in Cattle Dung Biochar-Packed Colocasia Esculenta-Based Vertical Subsurface Flow Constructed Wetland. *J. Water Process Eng.* **2021**, *41*, 101994, doi:10.1016/j.jwpe.2021.101994.
69. El Hamouri, B.; Nazih, J.; Lahjouj, J. Subsurface-Horizontal Flow Constructed Wetland for Sewage Treatment under Moroccan Climate Conditions B. *Desalination* **2007**, *248*, 123–130, doi:10.1016/j.desal.0000.00.000.
70. Gholipour, A.; Fragoso, R.; Galvão, A.; Duarte, E. Water Balance Analysis in a Novel Pilot-Scale of the Worm-Sludge Treatment Reed Bed (W-STRB) Planted with Arundo Donax. *Water Res.* **2024**, *250*, doi:10.1016/j.watres.2023.121066.

 doi:10.20944/preprints202604.2002.v1

71. Avellán, T.; Gremillion, P. Constructed Wetlands for Resource Recovery in Developing Countries. *Renew. Sustain. Energy Rev.* **2019**, *99*, 42–57, doi:10.1016/j.rser.2018.09.024.
72. Białowiec, A.; Albuquerque, A.; Randerson, P.F. The Influence of Evapotranspiration on Vertical Flow Subsurface Constructed Wetland Performance. *Ecol. Eng.* **2014**, *67*, 89–94, doi:10.1016/j.ecoleng.2014.03.032.
73. Chazarenc, F.; Naylor, S.; Comeau, Y.; Merlin, G.; Brisson, J. Modeling the Effect of Plants and Peat on Evapotranspiration in Constructed Wetlands. *Int. J. Chem. Eng.* **2010**, doi:10.1155/2010/412734.
74. Tuttolomondo, T.; Licata, M.; Leto, C.; Leone, R.; La Bella, S. Effect of Plant Species on Water Balance in a Pilot-Scale Horizontal Subsurface Flow Constructed Wetland Planted with Arundo Donax L. and Cyperus Alternifolius L. - Two-Year Tests in a Mediterranean Environment in the West of Sicily (Italy). *Ecol. Eng.* **2015**, *74*, 79–92, doi:10.1016/j.ecoleng.2014.10.020.